PROCEEDINGS OF SCIENCE

Preliminary elemental spectra from protons to iron nuclei with ISS-CREAM

Kenichi Sakai *,[a,b,*] **Yu Chen,**[c] **Stephane Coutu,**[c] **Jason T. Link,**[d] **John W. Mitchell,**[a] **S. A. Isaac Mognet,**[c] **Scott L. Nutter,**[e] **Jacob Smith**[f] **and Monong Yu**[g]

[a] *NASA Goddard Space Flight Center, Astroparticle Physics Laboratory, Greenbelt, MD 20771, USA*

[b] *Center for Research and Exploration in Space Science and Technology (CRESST), UMBC, Baltimore MD, 21250, USA*

[c] *Penn State University, Department of Physics, University Park, PA 16802, USA*

[d] *Laboratory for Atmospheric and Space Physics, University of Colorado, Boulder, CO 80303 USA*

[e] *Northern Kentucky University, Department of Physics, Geology, and Engineering Technology, Highland Heights, KY 41099 USA*

[f] *George Mason University, resident at U.S. Naval Research Laboratory, Washington, DC 20375, USA*

[g] *Institut de Física d'Altes Energies (IFAE), 08193 Bellaterra, Barcelona, Spain*

E-mail: kenichisakai@uchicago.edu

The ISS-CREAM experiment aims to measure spectra of cosmic-ray particles up to 1000 TeV from protons to iron nuclei. The detector was designed to complement other current space-based cosmic-ray missions and was installed on the ISS on August 22, 2017. During 539 days of on-orbit operations, ISS-CREAM recorded over 58 million events. Various subsystem issues occurred during on-orbit operations, reducing the period of stable operation of a 4-layer silicon charge detector and a tungsten/scintillating-fiber sampling calorimeter to about 225 live days. The development of more extensive calibrations is currently in progress to address the significant systematic errors associated with energy determination. We report preliminary elemental spectra of protons and helium, carbon, oxygen, neon, magnesium, silicon, and iron nuclei.

38th International Cosmic Ray Conference (ICRC2023)
26 July - 3 August, 2023
Nagoya, Japan

*Present address: Enrico Fermi Institute of The University of Chicago, Chicago, IL 60637, USA.
*Speaker

PoS(ICRC2023)136

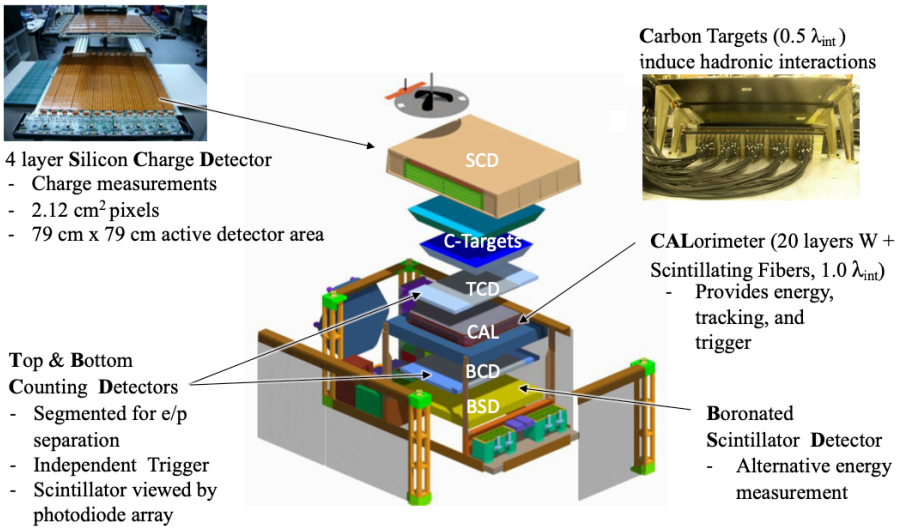

Figure 1: 3D view of the ISS-CREAM instrument

1. Introduction

Direct measurements of the high-energy spectra of each species of cosmic-ray nuclei provide detailed insight into the general phenomenology of cosmic-ray acceleration and propagation in the Galaxy. Several features in the cosmic-ray spectrum have been identified, including the so-called knee at a few times 10^6 GeV, the second knee at a few times 10^8 GeV, and a spectral steepening above 10^{11} GeV. In addition to these famous features, PAMELA claimed the existence of an additional break in the proton spectrum at $\sim$ 200 GeV [1]. This break was recently confirmed by many experiments like CREAM [2, 3], AMS-02 [4], ATIC-2 [5], CALET [6], DAMPE [7], and ISS-CREAM [8] , and was also observed in nuclei heavier than H (around 200 GeV/n). This spectral hardening has not been understood yet, and is thought to be a good probe for modeling of the cosmic-ray acceleration and transport properties in different regions of the Galaxy, a local effect of nearby supernova remnants, or reacceleration by weak shocks.

2. ISS-CREAM instrument

The ISS-CREAM experiment, illustrated in Figure 1, was developed based on a balloon-borne instrument, CREAM, which has measured the fluxes of elements between protons and iron in an energy region nearly up to the knee [9]. As cosmic-ray nuclei enter the instrument, their charge is determined with multiple layers of a silicon detector, the SCD [10]. For some nuclei, a hadronic interaction takes place in the carbon targets, and the shower energy is measured in a 20 layer tungsten-scintillating fiber tracking calorimeter, or CAL. ISS-CREAM includes other detectors not

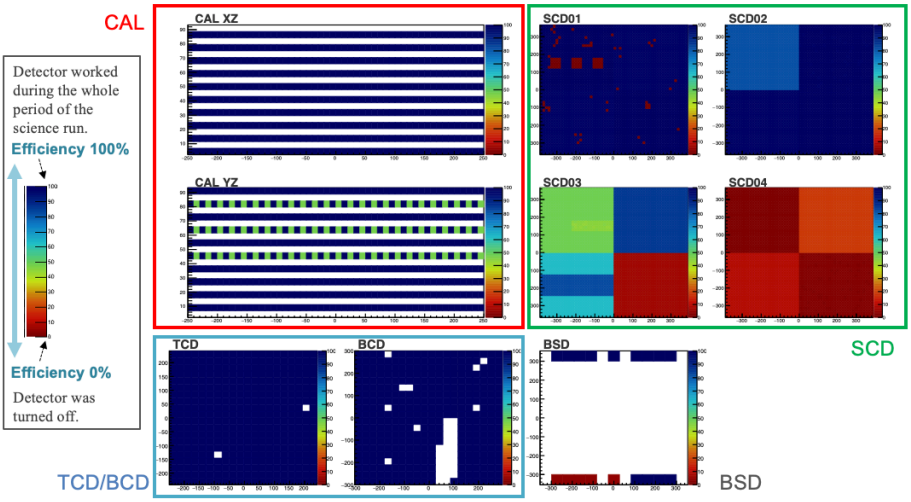

Figure 2: Detection efficiencies of each detector defined by HV status. See text for details.

flown on the balloon instrument. The Top and Bottom Counting Detectors, or TCD and BCD, are placed directly above and below the calorimeter, respectively, and give additional shower position measurements as well as providing an instrument trigger [11, 12]. A boronated scintillator detector, or BSD, located underneath the BCD, completes the detector stack, and provides an alternative energy measurement [13].

3. Detection efficiencies of each detector during observations

ISS-CREAM was launched in August 2017 on a SpaceX Falcon rocket in the trunk of the Dragon module and installed on the Japanese Experiment Module - Exposed Facility (JEM-EF) where it was operated until February 2019. For the first year, detector voltages were turned off during South Atlantic Anomaly (SAA) transits. After one year of operations, the instrument was always on, even through the SAA, except for a few short down-periods.

In this work, we required a very strict set of quality criteria in the data for calculating the preliminary fluxes. The science observations of 325 days during the on-orbit operations resulted in 225 live days by trimming the periods when no HV was applied to the CAL or when the total number of channels per event was abnormally high (indicative of noise).

Figure 2 shows efficiencies of each detector operated during the science run of 225 days. Channels that worked during the whole period of the science run have an efficiency of 100%, relative to the 225 days of CAL operation. Half of the channels in 3 layers of the CAL have an efficiency of about 50%. The top two layers of the SCD operated well, but the bottom two SCD layers have low efficiency. In particular, SCD4 was extremely noisy and was turned off for much of

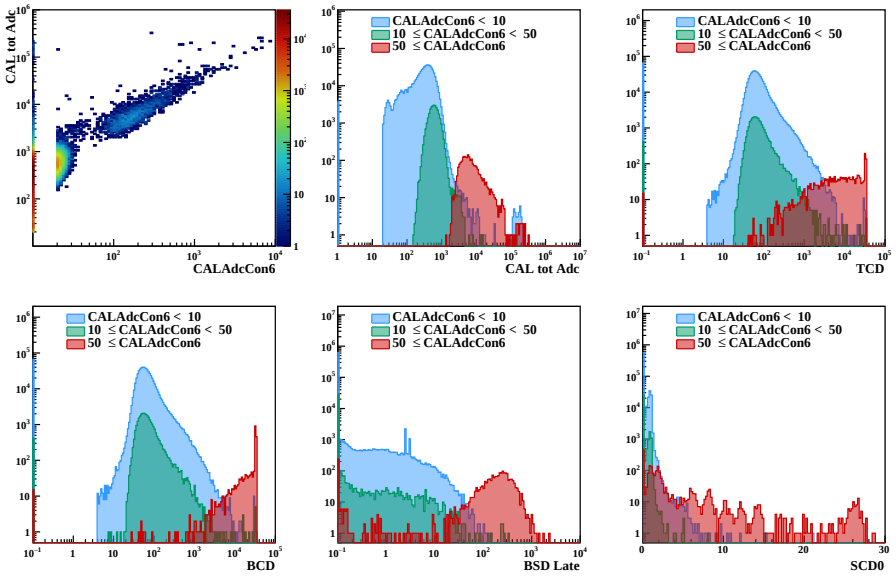

Figure 3: (Upper left) The total ADC in the CAL vs CALAdcCon6. (Other panels) The raw ADCs for the CAL, TCD, BCD, BSD, and SCD were divided into red histograms (50 ≤ CALAdcCon6), green histograms (10 ≤ CALAdcCon6 < 50), and blue histograms (CALAdcCon6 < 10).

the flight. Though the TCD was stable, the BCD had a significant dead zone (clear regions in the figure). In the BSD, 13 out of 18 photomultiplier tubes (PMTs) operated stably after a failure of the other 5 shortly after deployment to the ISS.

4. Separation of noise and cosmic-ray events

Checking the response of the detector reveals that events triggered by cosmic rays are difficult to distinguish from noise and pedestal calibration events. This made it very difficult to separate cosmic rays from noise events in the ISS-CREAM data analysis, but applying an ADC threshold cut on 6 consecutive layers in the CAL (CALAdcCon6) worked very effectively. This software cut mimics the hardware trigger requirement for high energy events, effectively eliminating noise events. The upper left panel of Figure 3 shows the total ADC in the CAL vs CALAdcCon6 after requiring fiducial cuts so that the track passes through all detectors in the science events triggered by the CAL. A clear gap exists around CALAdcCon6 = 50, dividing the data in two. With this distinction, the raw ADCs for the five detectors show markedly different distributions (Figure 3). The statistics drop to 0.3% of events triggered by the CAL during 225 days of live time, but for all detectors, the cut with CALAdcCon6 ≥ 50 is efficient in selecting cosmic-ray events. In preliminary flux calculations, a CALAdcCon6 ≥ 50 cut was adopted.

5. CAL calibration

The difficulty with the CAL calibration derives from the fact that the design of the ISS-CREAM instrument is dedicated to the observation of ultra-high energy cosmic rays and cannot trigger on

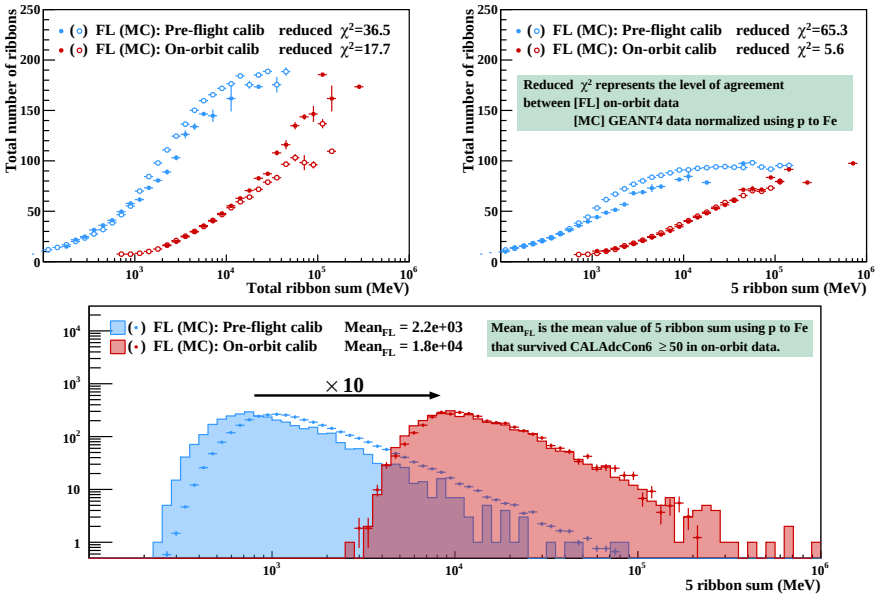

Figure 4: (Upper panels) The total number of ribbons assigned for tracking and the total energy deposit in the selected ribbons. (Lower panel) Absolute energy calibration from the pre-flight beam test (blue histogram) to the new calibration using the on-orbit data (red histogram).

non-shower events. Essentially, the ADC of the CAL is converted to ionization loss (MeV) by using the calibrated parameters from a pre-flight beam test. This test was performed with CREAM electronics, which varied significantly in gain from the ISS-CREAM electronics. A reasonable extrapolation of the beam test calibrations to the ISS-CREAM calorimeter electronics led to fluxes two orders of magnitude below those measured by other experiments.

An energy calibration was developed by aligning the profiles of showers developing in the CAL with the on-orbit data and Monte Carlo (MC) predictions. Since the CAL is very noisy so that experimental distributions are nearly impossible to reproduce in MC, only a small portion of the CAL fiber ribbons around the track was used for calibration to minimize the uncertainty arising from the noisy channels. The upper panels of Figure 4 show the total number of ribbons assigned for tracking and the total energy deposit in the selected ribbons, when using all ribbons (upper left) and when using only 5 ribbons around the track (upper right) in all events, including protons to iron nuclei. We see that the on-orbit data are a better match with the MC with only 5 ribbons around the track than with all ribbons. Figure 4 indicates a significant improvement from pre-flight beam test calibration to the new CAL calibration based on a limited number of ribbons.

This approach results in an energy calibration shift that seems unreasonably large. In fact, there is as much as a factor of 10 difference between the beam test calibration and the latest calibration using the on-orbit data, as shown in the lower panel of Figure 4. The CALET experiment, also on the ISS and with a calorimeter, carefully discussed the energy shift of 3.5% between the reconstructed energy from the MC tuned by an accelerator beam test data and the energy from the analysis of the geomagnetic cutoff [14]. By comparison, we are seriously considering why the energy shift is a factor of 10 in ISS-CREAM. This absolute energy calibration is controversial, and the systematic errors have not been investigated in detail yet.

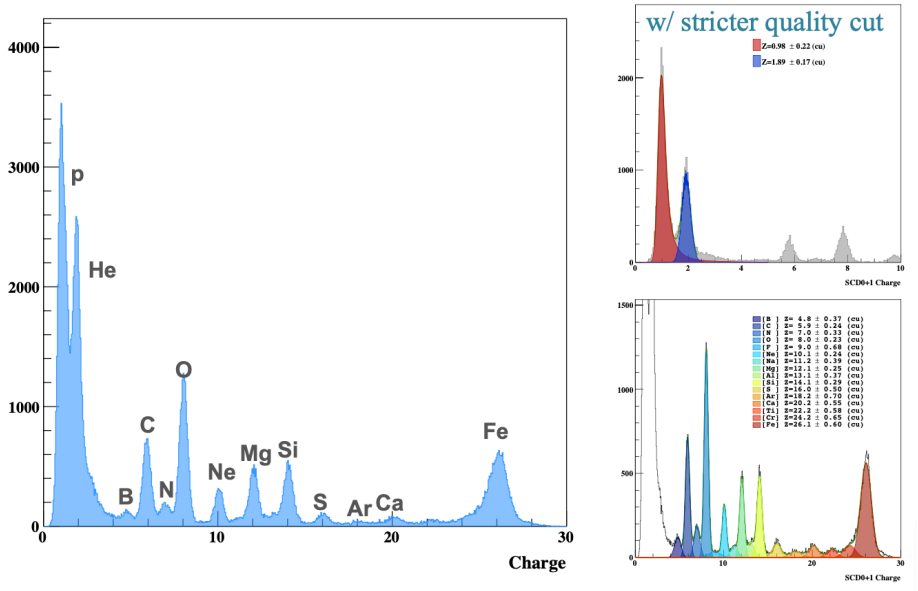

Figure 5: SCD charge distribution by using the average signal in the top two layers (left) based on new SCD/TCD/CAL-based tracking. Charge peak fits are shown for protons and helium (top right), and for Z from 6 to 26 (bottom right).

6. SCD calibration

The measured charge distribution up to iron is shown in Figure 5. The charge was determined by the average signal in the top two SCD layers. While strict cuts are used to separate protons from helium, much looser selection cuts are used to obtain higher statistics for heavier nuclei. The achieved charge resolution is 0.23 e for protons, and worsens with Z, up to 0.60 e for iron nuclei.

7. Preliminary fluxes from protons to iron nuclei

In the flux determination, quality cut efficiencies were calculated on an independent sample selected using a likelihood derived using machine learning analysis. A Geant4 MC simulation provided the geometrical acceptances and was used to estimate the contamination due to background events. The conversion from energy deposit in the CAL to energy of the incident particle was performed with an unfolding procedure using Bayesian statistics with a response function generated with Geant4.

Figure 6 shows preliminary elemental spectra from protons to iron nuclei with this ISS-CREAM analysis compared to CREAM [3, 15], HEAO 3-C2 [16], TRACER [17], PAMELA [1, 18], AMS-02 [4, 19–22], DAMPE [7, 23], CALET [6, 24, 25] and an independent ISS-CREAM analysis [8]. The resulting fluxes in this work (red dots) have only statistical errors and the higher energy region is determined by requiring a minimum of two events in each bin.

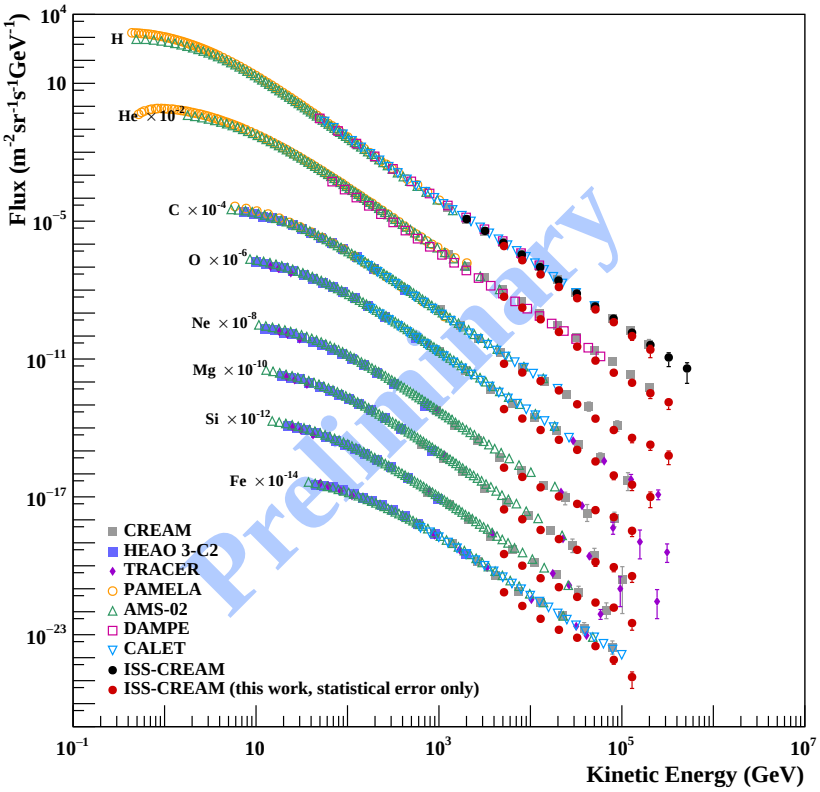

Figure 6: Preliminary elemental spectra from protons to iron nuclei in the present ISS-CREAM analysis compared to CREAM [3, 15], HEAO 3-C2 [16], TRACER [17], PAMELA [1, 18], AMS-02 [4, 19–22], DAMPE [7, 23], CALET [6, 24, 25] and an independent ISS-CREAM analysis [8].

The high-energy flux points exhibit a systematic bumpy structure, which is determined by the number of unfolding iterations used. The MC-generated response function used in the unfolding assumes a specific power index. Four iterations are used in the unfolding process. Reducing the number of iterations is a good way to prevent the bias in the flux shape due to the unfolding, though this might result in artificially shifting the index, so a more systematic study is essential and planned.

8. Conclusion

Analysis of ISS-CREAM data is ongoing. At this time, the systematic errors resulting from the absolute energy calibration are expected to be very large, and we are developing a calibration method with smaller uncertainties. The secondary-to-primary ratio analysis, in which many systematic errors can be ignored, has also been performed in parallel, as discussed elsewhere [26].

Acknowledgements

This work was supported in the U.S. by NASA grants NNX17AB43G, NNX17AB42G, and their predecessor grants, as well as by directed RTOP funds to NASA GSFC. The authors also thank M. Geske, Penn State, for contributions to the BSD, and K. Wallace at Northern Kentucky University for contributions to Monte Carlo simulations. We also recognize the contributions of past CREAM and ISS-CREAM collaborators.

References

[1] O. Adriani *et al.*, Science **332**, 69 (2011).
[2] Y. S. Yoon *et al.*, The Astrophysical Journal **728**, 122 (2011).
[3] Y. S. Yoon *et al.*, The Astrophysical Journal **839**, 5 (2017).
[4] M. Aguilar *et al.*, Phys. Rev. Lett. **114**, 171103 (2015).
[5] A. D. Panov *et al.*, Bulletin of the Russian Academy of Sciences: Physics **73**, 564 (2009).
[6] O. Adriani *et al.*, Phys. Rev. Lett. **122**, 181102 (2019).
[7] Q. An *et al.*, Science Advances **5**, 10.1126/sciadv.aax3793 (2019).
[8] G. H. Choi *et al.*, The Astrophysical Journal **940**, 107 (2022).
[9] E. Seo *et al.*, Advances in Space Research **53**, 1451 (2014).
[10] J. Lee *et al.*, Astroparticle Physics **112**, 8 (2019).
[11] H. Hyun *et al.*, Nucl. Inst. and Methods A **787**, 134 (2015).
[12] S. Kang *et al.*, Advances in Space Research **64**, 2564 (2019).
[13] Y. Amare *et al.*, Nucl. Inst. and Methods A **943**, 162413 (2019).
[14] O. Adriani *et al.*, Phys. Rev. Lett. **119**, 181101 (2017).
[15] H. S. Ahn *et al.*, The Astrophysical Journal **707**, 593 (2009).
[16] J. J. Engelmann *et al.*, Astron. Astrophys. **233**, 96 (1990).
[17] M. Ave *et al.*, The Astrophysical Journal **678**, 262 (2008).
[18] O. Adriani *et al.*, The Astrophysical Journal **791**, 93 (2014).
[19] M. Aguilar *et al.*, Phys. Rev. Lett. **115**, 211101 (9pp) (2015).
[20] M. Aguilar *et al.*, Phys. Rev. Lett. **119**, 251101 (2017).
[21] M. Aguilar *et al.*, Phys. Rev. Lett. **124**, 211102 (2020).
[22] M. Aguilar *et al.*, Phys. Rev. Lett. **126**, 041104 (2021).
[23] F. Alemanno *et al.*, Phys. Rev. Lett. **126**, 201102 (2021).
[24] O. Adriani *et al.*, Phys. Rev. Lett. **125**, 251102 (2020).
[25] O. Adriani *et al.*, Phys. Rev. Lett. **126**, 241101 (2021).
[26] Y. Chen *et al.*, ICRC2023 PCRD0-02, these proceedings .